ENGINEERING TRANSACTIONS • Engng. Trans. • 41, 2, 187–208, 1993
Polish Academy of Sciences • Institute of Fundamental Technological Research

NATURAL CONVECTION IN A CYLINDRICAL CAVITY HEATED BY AN INTERNALLY-LOCATED STRONG SOURCE

J. SŁOMCZYŃSKA (WARSZAWA)

Stationary natural convection caused by a strong source of heat centrally located in a cylindrical cavity is analyzed by a finite-difference method. Since gradients of pressure are much smaller than gradients of both the temperature and density, the axisymmetric flow is treated as incompressible while, for the same reason, variable density is fully accounted for. Viscosity and thermal conductivity are assumed to be functions of temperature. Coupled stationary equations of continuity, motion, and energy are formulated in the framework of primitive variables. Line integration of the equation of motion over a closed contour is used to eliminate pressure. The solution, i.e. temperature (hence, density) and velocity distributions in the cavity, is found by a two-step iterative procedure based on line succesive overrelaxation. Examples of computation showing the effects of change in the source heat-rate, mean value of pressure and the aspect ratio of the cavity are provided.

1. INTRODUCTION

Steady progress in developing computational equipment and techniques for nonlinear partial differential equations accounts for the rapid growth in the number of studies devoted to natural and forced convection in physics and engineering applications. However, in spite of the great variety in the physical and mathematical models of convection as well as in the methods for seeking numerical solutions, only a few basic models of the heat source setting have been utilized.

The majority of papers devoted to buoyancy driven, laminar natural convection in immobile cavities pertain to situations in which heat is transferred to the cavity by an isothermal wall. Most often this is either a bottom wall of a cavity for which the onset, stability and flow patterns of the Rayleigh-Bénard convection are analyzed (e.g. STENGEL *et al.* [32], BLAKE *et al.* [3], ARTER [1], BUSSE and FRICK [4]), or a vertical wall of a cavity

for which the dependence of the flow pattern upon the aspect ratio is studied (e.q. QUON [23], KNIGHT and PALMER [13], LEE and KORPELA [15], PHILLIPS [21], LE QUERE and DE ROQUEFORT [22]). Less frequently considered are convection models with different ways of wall heating, e.g. with temperature changing along the wall (MALLINSON *et al.* [16], GILLY *et al.* [8], WALTON [33]), a differentially heated corner of the cavity (KIMURA and BEJAN [12]), time periodic heating (ROPPO *et al* [28]), or with the source of heat moving along the wall (RAMARAJU *et al.* [24]). Modelling the source of heat inside the cavity is seldom done and almost exclusively limited to problems involving combustion (e.g. O'ROURKE and BRACCO [19]). KARWE and JALURIA [11] considered a different example of convection due to an internal source but that source was not strong enough to produce high gradients of temperature and density.

This paper focusses on convection in a laser chamber, caused by a strong stationary source of heat located in the center of the cavity. An unusual modelling of the heat-source setting necessitates modifications of the relationship among the main variables. The source generates high temperature and density gradients while the spatial changes of pressure are considerably smaller. Because of highly variable density, the Boussinesq approximation, which is standard for incompressible problems, cannot be used. Therefore, even though the flow is considered to be incompressible, variable density makes the method developed for obtaining the numerical solution similar in this respect to the methods used in compressible studies.

2. ASSUMPTIONS, EQUATIONS AND GENERAL STRATEGY FOR OBTAINING THE SOLUTION

We present and discuss a model of natural convection in a laser chamber during a continuous optical discharge. A small volume of high temperature plasma is maintained by a strong focussed laser beam for a sufficiently long duration to consider a stationary effect (GENERALOV *et al.* [7], KOZLOV *et al.* [14], MOODY [17]). Since the plasma is centered in the chamber and relatively small, we represent the chamber as a cylinder and define the problem as axially symmetric. The most important other physical feature is that the strong heat source causes high temperature and density gradients in the flow of viscous gas around the plasma, while pressure in the cavity remains nearly uniform (MUCHA *et al.* [18], BARANOWSKI *et al.* [2]). There-

fore, we treat the gas as incompressible. Specifically, we assume that local changes of density depend solely on temperature and not on the pressure. A nonuniform density distribution must be fully considered ($\rho_{\max}/\rho_{\min} \approx 40$). Therefore, contrary to common practice in the analysis of incompressible flows, the velocity field is not treated as divergence-free.

Similarity analysis of the momentum and energy equations of a compressible flow at small Mach numbers shows that spatial fluctuations of pressure are negligible in equations of energy and state. So is the dissipation function in the energy equation (O'ROURKE and BRACCO [19]). Thus, in our model of a stationary incompressible flow we simplify the energy equation by dropping the pressure term and the dissipation function. Of course, the pressure gradient cannot be neglected in the equation of motion. The constitutive relationship among thermal variables is provided by the equation of state for perfect gas in which the mean (i.e. volume averaged) rather than local value of pressure is used (O'ROURKE and BRACCO [19]).

In Cartesian coordinates (x_1, x_2, x_3) covering the cylindrical domain $\Omega \subset \mathbf{R}^3$ equations that specify the problem under consideration are

$$\frac{\partial}{\partial x_\mu}(\rho v^\mu) = 0, \tag{2.1}$$

$$\rho v^\mu \frac{\partial v^\nu}{\partial x_\mu} = -\frac{\partial p}{\partial x_\nu} + \frac{\partial}{\partial x_\mu}\left\{\eta\left(\frac{\partial v^\nu}{\partial x_\mu} + \frac{\partial v^\mu}{\partial x_\nu}\right)\right\} + \frac{\partial}{\partial x_\nu}\left\{\left(\zeta - \frac{2}{3}\eta\right)\frac{\partial v^\alpha}{\partial x_\alpha}\right\} + \rho g^\nu, \tag{2.2}$$

$$c_p \rho v^\mu \frac{\partial T}{\partial x_\mu} = \frac{\partial}{\partial x_\mu}\left(\kappa \frac{\partial T}{\partial x_\mu}\right) + q, \tag{2.3}$$

$$\overline{p} = \rho R T, \tag{2.4}$$

where $\mu, \nu, \alpha = 1, 2, 3$, $\mathbf{x} = (x_1, x_2, x_3) \in \Omega \subset \mathbf{R}^3$, $v^\nu(\mathbf{x})$ – ν^{th} component of gas velocity, $p(\mathbf{x})$ – pressure, with $\overline{p}$ being its mean value in Ω, $\rho(\mathbf{x})$ – density, $\eta(\mathbf{x})$ – dynamic viscosity, $\zeta(\mathbf{x})$ – bulk viscosity, g^ν – ν^{th} component of acceleration of gravity, c_p – specific heat at constant pressure, $T(\mathbf{x})$ – gas temperature, $\kappa(\mathbf{x})$ – thermal conductivity, $q(\mathbf{x})$ – source heat-rate per unit volume, R – the gas constant. Coefficients of viscosity and thermal conductivity are assumed to be known functions of temperature.

Pressure – appearing in the momentum equations – is a rather cumbersome variable. In numerical schemes involving pressure explicitly, the distribution of this variable is usually found as a solution to a Poisson equation,

derived from the momentum equations. One of the difficulties in solving this equation stems from the lack of natural boundary conditions.

Neumann homogeneous boundary conditions, usually adopted in this case, are sometimes inconvenient for physical (HIRSCHEL and GROH [9]) and computational (RUBIN [29], LE QUERE and DE ROQUEFORT [22]) reasons. Moreover, incorporating the Poisson equation for pressure normally leads to the continuity equation being satisfied only indirectly. This, in turn, may result in poor convergence if the global compatibility condition for the pressure gradient normal to the boundary is not accurately satisfied (RUBIN [29]). In low-Mach-number compressible flow problems with small pressure inhomogeneities there are still other pressure-related difficulties involving inefficiency of computation (RAMSHAW *et al.* [25]).

In the analysis of two-dimensional incompressible flows the usual way to avoid dealing directly with pressure is to formulate the problem in the vorticity-stream function framework. In this framework, uncoupling pressure is accomplished by having the momentum equation replaced with the vorticity-transport equation. If density is constant, the new equation is easier to handle because the basic terms involving the main variable (i.e. vorticity in the vorticity-transport equation and velocity in the momentum equation) are the same as in the original equation, while pressure is eliminated. Variable density makes this framework much less attractive (ROACHE [27]). Although pressure can still be eliminated by replacing primitive variables with vorticity and stream function, this is accomplished at the cost of many new terms appearing in the vorticity-transport equation (e.g. INABA and FUKUDA [10]).

With no clear gain to follow from applying the vorticity-stream function framework to our problem, we retain primitive variables. Nevertheless, pressure is eliminated as an active variable. Elimination is based on the Stokes theorem from which it immediately follows that a line integral of a gradient, taken over a closed contour, vanishes identically[(1)]. Thus, an integration of the momentum equation over any closed contour results in eliminating both of its gradient terms (which contain pressure and bulk

[(1)] Let F be any function with all first and second derivatives in $\Omega \subset \mathbf{R}^3$. Let S be a surface in Ω which can be oriented by a unit normal vector $\mathbf{n}$ at each point of S with $\mathbf{n}$ continuous over S. Let c be the contour of S and $\boldsymbol{\tau}$ be a unit vector tangent at each point of c and continuous over c. The Stokes theorem, applied to function $\mathbf{G} = \nabla F$, provides

$$\int_c \nabla F \cdot \boldsymbol{\tau}\, dl = \iint_S (\operatorname{curl} \nabla F) \cdot \mathbf{n}\, d\sigma = 0.$$

viscosity). Accordingly, we replace Eq. (2.2) with

$$\int_c \mathcal{L}^\nu \tau_\nu \, d\tau_\nu = 0, \qquad \nu = 1,2,3. \tag{2.2'}$$

where $\boldsymbol{\tau} = (\tau_1, \tau_2, \tau_3)$ is a unit vector tangent to the closed contour c and the integrand $\boldsymbol{\mathcal{L}}$ is composed of three terms of the original equation (convective; viscous; buoyancy).

Having formulated the problem in terms of primitive variables, we set simple and physically straightforward boundary conditions for velocity and temperature. We assume the velocity vector to vanish at the boudary $\partial\Omega$ while temperature remains constant. There is no equally good justification in physical terms for the boundary conditions for other variables. Therefore, we have chosen them as compatibility conditions, assuring that all equations would be satisfied at the boundary. Accordingly, conditions for density are set to satisfy Eq. (2.4) while values of viscosity and thermal conductivity are taken from appropriate tables of gas properties, as corresponding to the boundary value of temperature. Hence, boundary conditions for all variables are of the Dirichlet type.

Equations (2.1)–(2.4) are nonlinear and coupled, therefore requiring some iteration. To limit the memory storage we chose to use a full-scale iterative method. In our double-loop iterative scheme the convection problem is split into two partial problems denoted as T (for temperature) and N-S (for Navier–Stokes). In each (outer) iteration the last solution of one subproblem (obtained through inner iterations) serves as data for the other subproblem, and iterations are continued until a satisfactory convergence is obtained. Since the method for solving the Navier–Stokes problem has been presented in some detail in an earlier work (SŁOMCZYŃSKA and PERADZYŃSKI [30]) while the procedure for solving the full convection problem was only briefly outlined elsewhere (SŁOMCZYŃSKA [31]), this paper stresses the temperature problem.

Sequence of computation in k-th iteration for the full convection problem:

T problem	$\overset{(k-1)}{\mathbf{v}}, \overset{(k-1)}{\rho}, \overset{(k-1)}{\kappa} \xrightarrow{(3)} \overset{(k)}{\mathrm{T}}$ $\overset{(k)}{\mathrm{T}} \xrightarrow{(4)} \overset{(k)}{\rho}$ $\overset{(k)}{\mathrm{T}} \xrightarrow{\text{tables of properties}} \overset{(k)}{\eta}, \overset{(k)}{\kappa}$
N – S problem	$\overset{(k)}{\rho}, \overset{(k)}{\eta} \xrightarrow{(1),(2^*)} \overset{(k)}{\mathbf{v}}$

3. Discretization and the numerical procedure

We solve the outlined problem by means of as iterative finite-difference method. The governing equations are normalized and expressed in the conservation form, particularly recommended for problems with variable density (e.q. ROACHE [26]). They are then integrated over a cylindrical control volume V_Σ bounded by a pair of planes $z = z_i$, $z = z_{i+1}$, a pair of cylindrical surfaces $r = r_j$, $r = r_{j+1}$, and a pair of planes $\phi = \phi_k$, $\phi = \phi_{k+1}$. From the Gauss theorem it follows that the equation of energy, integrated over V_Σ, becomes

$$\int_{\partial V_\Sigma} \left(\rho v^\mu T - \frac{\kappa}{\mathrm{Pe}} \frac{\partial T}{\partial x_\mu}\right) n_\mu \, d\sigma = Q_{ns}, \tag{3.1}$$

where $\mathrm{Pe} = (c_p \rho_b u_b L_b)/\kappa_b$ – the Peclet number, $Q_{ns}(i,j) = Q/(c_p T_b \rho_b u_b L_b^2)$ – the source nondimensional heat rate supplied to the control volume, $\mathbf{n} = (n_1, n_2, n_3)$ – a unit vector normal to the boundary ∂V_Σ, L_b, u_b, ρ_b, T_b, κ_b – characteristic (dimensional) quantities.

To account for the cylindrical symmetry Eq. (3.1) must be expressed in cylindrical coordinates (r, ϕ, z). Considering appropriate relations between the Cartesian and the cylindrical coordinate systems under axial symmetry $(\partial \cdot / \partial \phi = 0,\ v^\phi = 0)$, we express the integrand in Eq. (3.1) as

$$\{(n_1 \cos\phi + n_2 \sin\phi)\rho u + n_3 \rho v\} T - \frac{\kappa}{\mathrm{Pe}} \left\{(n_1 \cos\phi + n_2 \sin\phi)\frac{\partial T}{\partial r} + n_3 \frac{\partial T}{\partial z}\right\},$$

where u and v denote v^r and v^z, respectively. To complete the integration over ∂V_Σ we notice that for surfaces (I) $r = \mathrm{const}$: $n_1 = \cos\phi$, $n_2 = \sin\phi$, $n_3 = 0$, $\partial\sigma = r\,d\phi\,dz$; (II) $\phi = \mathrm{const}$: $n_1 = -\sin\phi, n_2 = \cos\phi$, $n_3 = 0$, $\partial\sigma = dr\,dz$; and (III) $z = \mathrm{const}$: $n_1 = 0$, $n_2 = 0$, $n_3 = 1$, $\partial\sigma = r\,dr\,d\phi$. Hence

$$\left[r \int_{z_i}^{z_{i+1}} \left(\rho u T - \frac{\kappa}{\mathrm{Pe}} \frac{\partial T}{\partial r}\right) \int_{\phi_k}^{\phi_{k+1}} d\phi\, dz\right]_{r_j}^{r_{j+1}} + \left[\int_{z_i}^{z_{i+1}} \int_{r_j}^{r_{j+1}} -\frac{\kappa}{\mathrm{Pe}} \frac{\partial T}{r\partial\phi} dr\, dz\right]_{\phi_k}^{\phi_{k+1}}$$
$$+ \left[\int_{r_j}^{r_{j+1}} r \left(\rho v T - \frac{\kappa}{\mathrm{Pe}} \frac{\partial T}{\partial z}\right) \int_{\phi_k} d\phi\, \partial r\right]_{z_i}^{z_{i+1}} = Q_{ns}. \tag{3.2}$$

Since under axial symmetry $\partial T/\partial\phi = 0$, Eq. (3.2) reduces to the following two-dimensional equation in domain Ω_{2+} being a half-plane of the z-axial

cross-section of domain Ω

$$(3.3)\qquad \left[r\int_{z_i}^{z_{i+1}}\left(\rho uT-\frac{\kappa}{\mathrm{Pe}}\frac{\partial T}{\partial r}\right)dz\right]_{r_j}^{r_{j+1}}+\left[\int_{r_j}^{r_{j+1}} r\left(\rho vT-\frac{\kappa}{\mathrm{Pe}}\frac{\partial T}{\partial r}\right)dr\right]_{z_i}^{z_{i+1}}=\frac{Q_{ns}}{2\pi}.$$

A similar procedure applied to equations of continuity and motion (see SŁOMCZYŃSKA and PERADZYŃSKI [30] for derivation) provides

$$(3.4)\qquad \left[r\int_{z_i}^{z_{i+1}}\rho u\,dz\right]_{r_j}^{r_{j+1}}+\left[\int_{r_j}^{r_{j+1}} r\rho v\,dr\right]_{z_i}^{z_{i+1}}=0,$$

$$(3.5)\qquad \int_c S^\mu\tau_\mu\,d\tau_\mu=\mathrm{Re}\int_c P^\mu\tau_\mu\,d\tau_\mu,$$

where

$$(3.6)\qquad S^r(i,j)=2\left[r\int_{z_i}^{z_{i+1}}\eta\frac{\partial u}{\partial r}dz\right]_{r_j}^{r_{j+1}}+\left[\int_{r_j}^{r_{j+1}} r\eta\left(\frac{\partial u}{\partial z}+\frac{\partial v}{\partial r}\right)dr\right]_{z_i}^{z_{i+1}}-2r\int_{z_i}^{z_{i+1}}\int_{r_j}^{r_{j+1}}\eta\frac{u}{r}dr\,dz,$$

$$(3.7)\qquad S^z(i,j)=2\left[\int_{r_j}^{r_{j+1}} r\eta\frac{\partial v}{\partial z}dr\right]_{z_i}^{z_{i+1}}+\left[r\int_{z_i}^{z_{i+1}}\eta\left(\frac{\partial u}{\partial z}+\frac{\partial v}{\partial r}\right)dz\right]_{r_j}^{r_{j+1}},$$

$$(3.8)\qquad P^r(i,j)=\left[r\int_{z_i}^{z_{i+1}}\rho u^2\,dz\right]_{r_j}^{r_{j+1}}+\left[\int_{r_j}^{r_{j+1}} r\rho uv\,dr\right]_{z_i}^{z_{i+1}},$$

$$(3.9)\qquad P^z(i,j)=\left[r\int_{z_i}^{z_{i+1}}\rho uv\,dz\right]_{r_j}^{r_{j+1}}+\left[\int_{r_j}^{r_{j+1}} r\rho v^2\,dr\right]_{z_i}^{z_{i+1}}-V(i,j)g\overline{\rho}(i,j),$$

$V(i,j)=\pi(r_j+r_{j+1})(r_{j+1}-r_j)(z_{i+1}-z_i)$, $\mathrm{Re}=(\rho_b u_b L_b)/\eta_b$ – the Reynolds number.

Since c is the borderline of the mesh (i,j) – denoted as (i,j) for its left-bottom corner – vectors S^μ and P^μ $(\mu = r,z)$ appearing in Eq. (3.5) are not computed in the node (i,j) but in points $\alpha,\beta,\gamma,\delta$ which are centers of four faces bounding the mesh. Hence $\alpha = (i, j+1/2)$, $\beta = (i+1/2, j+1)$, $\gamma = (i+1, j+1/2), \delta = (i+1/2, j)$. Intervals of integration in Eqs. (3.6)–(3.9) are modified accordingly.

The half-discretized equations (3.3), (3.4), (3.5) have been derived from Eqs. (2.3), (2.1) and (2.2′) without considering how the variables are defined on the grid, what their profiles are between nodes and how the boundary conditions are set. To arrive at the final discretization formulae, by applying the mean-value theorem to integrals in Eqs. (3.3), (3.4), (3.5) all of these need to be specified. Figure 1 presents the two-dimensional domain Ω_{2+} covered by the grid. Velocity, density and viscosity are defined over the set of grid-nodes (points (i,j), $i = 0,\ldots,m+1$; $j = 0,\ldots,n+1$); therefore setting the boundary conditions is straightforward for these variables. Temperature and thermal conductivity are defined in mesh centers (points $(i+1/2, j+1/2)$, $i = 0,\ldots,m$; $j = 0,\ldots,n$). To set the Dirichlet boundary conditions for temperature (and thermal conductivity), additional temperature nodes are located on the boundary. Using two grids staggered with respect to each other for defining two main variables (T and $\mathbf{v}$) helps to

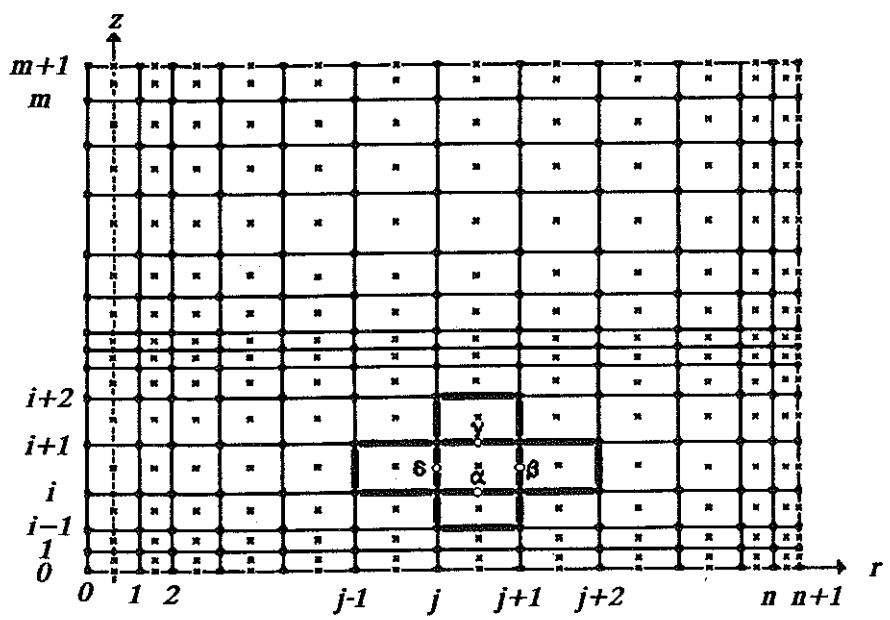

FIG. 1. Domain $\mathbf{Q}_{2+}$ covered by the grid. T and κ are defined in x-points, u, v, ρ and η are defined in ■-points.

develop discrete equivalents of all partial differential equations for the same mesh (i, j) without unnecessary interpolation. The discretized equation of continuity provides a relationship among variables (ρ and $\mathbf{v}$) defined in four nodes bounding the mesh (i, j), while the equation of energy links five centers of adjacent meshes providing a five-point formula for $T_{i+1/2,j+1/2}$, and the equation of motion – due to the linear integration over the mesh contour – links twelve nodes (cf. Fig. 1).

Before making assumptions about the between-node profiles of particular variables it is necessary to consider the fact that two of the differential equations are of the convection-diffusion type. The appearance of the first and second derivative in the convection-diffusion equation limits the stability of a numerical solution based on the central-difference representation of all derivatives (i.e. on the linear between-node profile of all variables appearing in the convective term) to low values of the cell Reynolds number ($R_c \leq 2$) (ROACHE [26], FROMM [6]). In practical computation this limitation is often found troublesome since it results in requiring the grid to be very fine. To overcome this difficulty COURANT *et al.* [5] developed a numerical scheme (upwind) free of the cell-Reynolds-number limitation, but, at the cost of reducing accuracy in representing the derivatives from the second to the first order. Subsequently, the upwind scheme has been often criticized for introducing artificial viscosity and therefore producing unrealistic numerical results. However, multiple versions of this scheme are very popular owing to their simplicity and effectiveness in problems with high values of R_c where the central-difference approach fails. Proponents of upwind schemes point to their positive features among which are the transportive property (ROACHE [26]) and a representation of the convection term which accounts for convection being an asymmetric phenomenon (PATANKAR [20]). Both these features are lacking in the central-difference approach although it produces second-order accurate representations of all derivatives.

The introduction of undesired artificial viscosity is a clearly negative feature of the upwind scheme. Therefore this scheme should be avoided if the solution of the problem is obtainable by the use of central differences. The equation of motion has been discretized in our method by applying central differences and the solution was obtained for many problems with $R_c > 2$. When the method was applied to the driven cavity problem, satisfactory solutions were obtained for $R_c = 15$. This was possible because of a partial cancellation of terms occurring in the discrete representation of the line integral of the convective term.

To show that some terms cancel in the line integral of the convective term of the equation of motion, we consider a simple example. The line integral is replaced by the curl operator, its numerical equivalent for integrating over the mesh boundary. It is first assumed that density is constant. Terms resulting from the density being actually different form its mean value over the integration contour do not undergo cancellation. For simplicity, a two-dimensional flow in plane Cartesian geometry is considered with $\mathbf{v} = (u, v)$ being the velocity vector, Ψ – the stream function, and ω – vorticity. The convective term and its curl are:

$$\begin{aligned} \mathbf{c} &= (\mathbf{v}\cdot\nabla)\mathbf{v} = \begin{pmatrix} u\,\partial u/\partial x + v\,\partial u/\partial y \\ u\,\partial v/\partial x + v\,\partial v/\partial y \end{pmatrix}, \\ \operatorname{curl}\mathbf{c} &= \mathbf{A} + \mathbf{B}, \end{aligned}$$

where

$$\begin{aligned} A &= \partial v/\partial x\,\partial u/\partial x + \partial v/\partial y\,\partial v/\partial x - \partial u/\partial x\,\partial u/\partial y - \partial u/\partial y\,\partial v/\partial y, \\ B &= u\,\partial^2 v/\partial x^2 + v\,\partial^2 v/\partial x\partial y - u\,\partial^2 u/\partial x\partial y - v\,\partial^2 u/\partial y^2. \end{aligned}$$

By introducing the stream function and vorticity, i.e. applying the formulae

$$u = \partial\Psi/\partial y, \qquad v = -\partial\Psi/\partial x, \qquad \omega = \partial u/\partial y - \partial v/\partial x,$$

we get $A = 0$, $B = -u\,\partial\omega/\partial x - v\,\partial\omega/\partial y$.

In meshes of constant vorticity curl $\mathbf{c}$ vanishes. Hence, for variable density, curl $\mathbf{c}$ contains only terms due to deviation of vorticity and density from their respective mean values over the contour of integration.

The energy equation was discretized following the scheme of PATANKAR [20]. The finite-difference formula for temperature in the center of the mesh (i, j) is

$$T_{i+1/2,j+1/2} = \frac{\alpha_1}{\alpha_0}T_{i+1/2,j+3/2} + \frac{\alpha_2}{\alpha_0}T_{i+3/2,j+1/2} + \frac{\alpha_3}{\alpha_0}T_{i+1/2,j-1/2} + \frac{\alpha_4}{\alpha_0}T_{i-1/2,j+1/2} + Q^*_{ij}, \tag{3.10}$$

where

$$\alpha_1 = (z_{i+1} - z_i)\frac{r_{j+1}}{r_{j+1/2}}\frac{\kappa_\beta}{\operatorname{Pe}(r_{j+3/2} - r_{j+1/2})} \times \{A(|P_\beta|) + \max(0; -P_\beta)\}, \tag{3.11}$$

$$\alpha_2 = (r_{j+1} - r_j)\frac{\kappa_\gamma}{\operatorname{Pe}(z_{i+3/2} - z_{i+1/2})}\{A(|P_\gamma|) + \max(0; -P_\gamma)\}, \tag{3.12}$$

$$\alpha_3 = (z_{i+1} - z_i)\frac{r_j}{r_{j+1/2}}\frac{\kappa_\delta}{\operatorname{Pe}(r_{j+1/2} - r_{j-1/2})} \times \{A(|P_\delta|) + \max(0; P_\delta)\}, \tag{3.13}$$

$$\alpha_4 = (r_{j+1} - r_j)\frac{\kappa_\alpha}{\operatorname{Pe}(z_{i+1/2} - z_{i-1/2})}\{A(|P_\alpha|) + \max(0; P_\alpha)\}, \tag{3.14}$$

α, β, γ, δ denote centers of faces bounding mesh (i,j) (cf. Fig. 1). P_ν, $\nu = \alpha, \beta, \gamma, \delta$, are values of the local Peclet number in these points, e.g.

$$P_\alpha = \mathrm{Pe}\frac{(\rho u)_\alpha (z_{i+1/2} - z_{i-1/2})}{\kappa_\alpha}. \tag{3.15}$$

In general A is a function of the local Peclet number. Its form depends on how the convective term is approximated by finite differences. For the central difference representation $A = 1 - 0.5|P_\nu|$. For the upwind scheme ($A = 1$) its value is independent of P_ν. For the hybrid scheme, using central differences for $P_\nu \leq 2$ and the upwind scheme elsewhere, we have $A(|P_\nu|) = \max(0; 1 - 0.5|P_\nu|)$. For Patankar's power-law scheme, providing a polynomial approximation of the expected exponential profile of the convection-propagated variable, $A(|P_\nu|) = \max\{0; (1 - 0.1|P_\nu|)^5\}$.

Numerical examples given in this paper were computed using the upwind option in formulae (3.11)–(3.15). Condition of axial symmetry ($\partial T/\partial r = 0$, $\partial \kappa/\partial r = 0$) is imposed by modifying Eqs. (3.11) and (3.13) for $j = 0$. Cylinder of radius r_1 is considered as the control volume. This results in setting the radius ratio in Eq. (3.11) equal to $0.5r_1$ and coefficient α_3 equal to zero.

Equation (3.10) is solved in the domain by line SOR. One mesh-block consists of meshes between two adjacent vertical lines j and $j+1$. Sweeps of ascending and descending orderings of j lines are iterated until satisfactory convergence is achieved. Local values of density are then calculated from the equation of state and local values of viscosity and thermal conductivity found from appropriate tables of properties. Computed T, ρ and η values are used as data for the N–S computation. The latter is performed in Ω_{2+} by a two-line SOR method which was designed for this purpose (SŁOMCZYŃSKA and PERADZYŃSKI [30]).

4. NUMERICAL RESULTS

The method discussed in this paper was applied to some problems of stationary natural convection in a cylindrical cavity heated by a centrally located cylindrical source supplying heat at a constant rate. Velocity was assumed to vanish at the boundary and temperature is constant and equal to 300 K. The height of the cavity was 4 cm and its diameter 3.6 cm in 7 cases out of 9 considered below. The source was modelled as a small cylinder, its height being 0.8 cm and its diameter 0.4 cm. A 21×21 nonhomogeneous

grid, with vertical lines concentrated in the vicinity of the z-axis, covered the right half of the z-axial section of the cavity. A rather coarse grid was chosen to allow for computation on a mini-computer.

The convergence criteria for both T and N-S partial problems were the maximal residual and the maximal difference in a node. When the ratio of each of these to the maximal value of temperature (or velocity in case of the N-S problem) fell below 10^{-5} (or 10^{-4} for the N-S problem), inner iterations were discontinued. Outer iterations were assumed to be convergent when 0.8 of the value of the inner criterion was achieved. The number of inner iterations varied from 30 (a preset maximum) to 1 for the T problem and from 50 to 1 for T the N-S problem. The number of outer iterations varied from 29 to 105 among solutions for nine data sets presented in this section. Temperature was overrelaxed with the factor $\omega = 1.2$. No overrelaxation was used for velocity. The nonlinear term in the momentum equation was underrelaxed with the factor $\nu = 0.1$.

Nine data sets – three for each particular problem – have been considered to show the effects of change in (1) the source heat-rate, (2) the mean value of pressure, and (3) the aspect-ratio of the domain. The results of computation are presented as temperature contours and streamlines.

In the first problem the rate of heat supplied to the cavity was 70 W (case a), 60 W (case b), and 50 W (case c). The mean value of pressure (1 ata), and the source and cavity dimensions were the same for all three cases. Figure 2 shows the temperature contours and Fig. 3 the streamlines in the right half cavity z-axial section. With a decreasing heat-rate (from 70 to 50 W) the maximal value of temperature decreased (from 13.564 to 10.621 K), and the maximal value of velocity rose (from 38.1 to 62.5 cm/s), as did the Reynolds number (from 92 to 120) and the Peclet number (from 2.3 to 3.6). A change in streamlines pattern occurs between the 70 W case – with two vortices, and the 60 W case – with one vortex.

The effect of change in the mean value of pressure – from 1 ata (case a) to 0.75 ata (case b) to 0.5 ata (case c) – is examined for the cavity of the same dimensions as in the first problem. The cavity is heated by a 60 W source. With the mean value of pressure decreasing (from 1 to 0.5 ata) $T_{\max}$ rose (from 12.250 to 12.640 K) and $v_{\max}$ decreased (from 45.5 to 21.0 cm/s). The Reynolds number decreased from 102 to 32 and the Peclet number from 2.6 to 0.8. The temperature contours (cf. Fig. 4) demonstrate the clearly diminishing effect of convection. The streamlines comparison (cf. Fig. 5) shows one vortex in the 1 ata case and two in the two remaining cases.

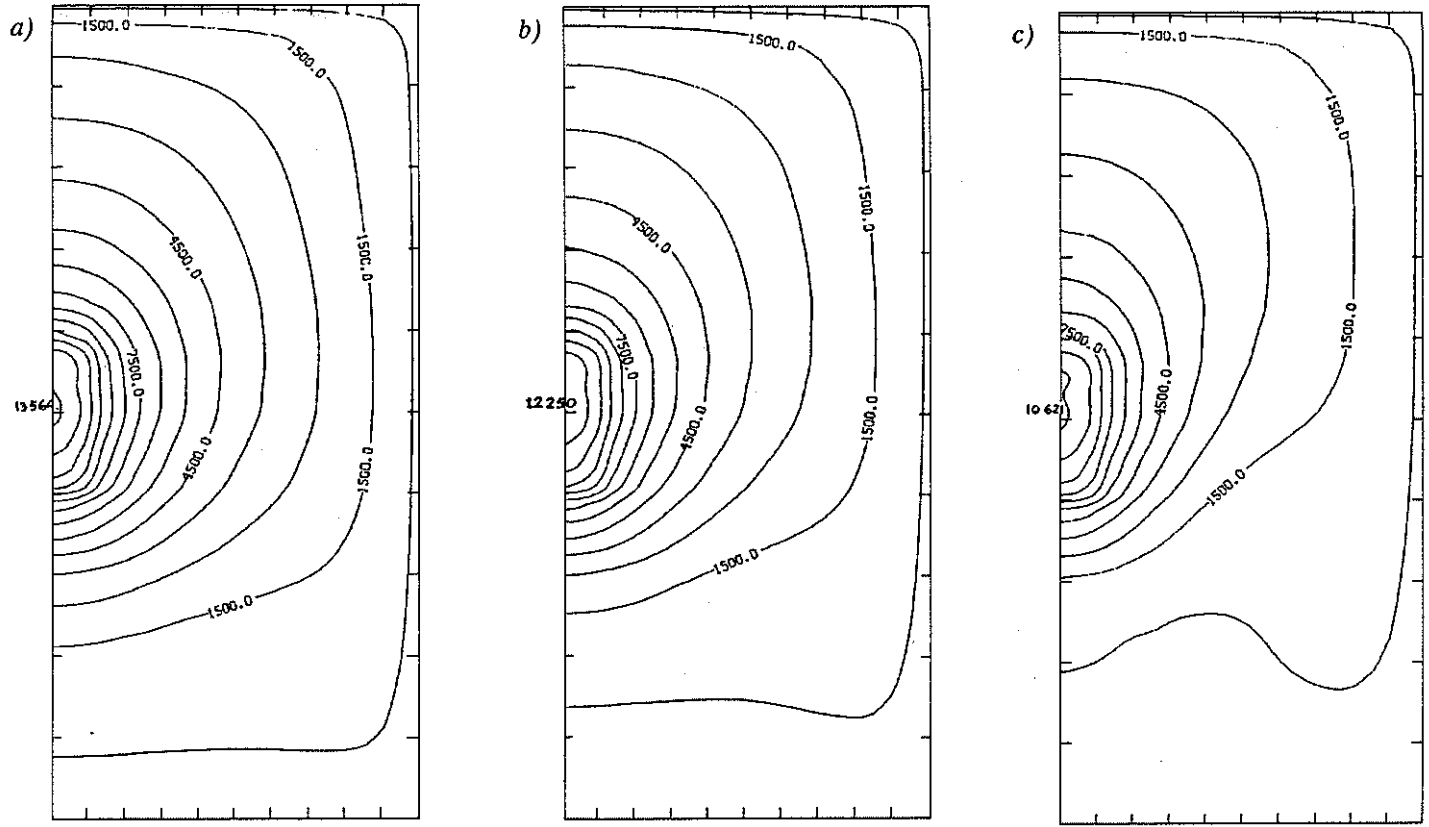

T_{max} = 13 564 K Re = 92
v_{max} = 38.1 cm/s Pe = 2.3

T_{max} = 12 250 K Re = 102
v_{max} = 45.5 cm/s Pe = 2.6

T_{max} = 10 621 K Re = 120
v_{max} = 62.5 cm/s Pe = 3.6

FIG. 2. Temperature contours for different values of source power: a) 70 W, b) 60 W, c) 50 W. Mean pressure: $\bar{p} = 1$ ata. Cavity dimensions: Radius: $R_d = 1.8$ cm, height: $Z_d = 4.0$ cm. Source dimensions: Radius: $R_Q = 0.2$ cm, height: $Z_Q = 0.8$ cm.

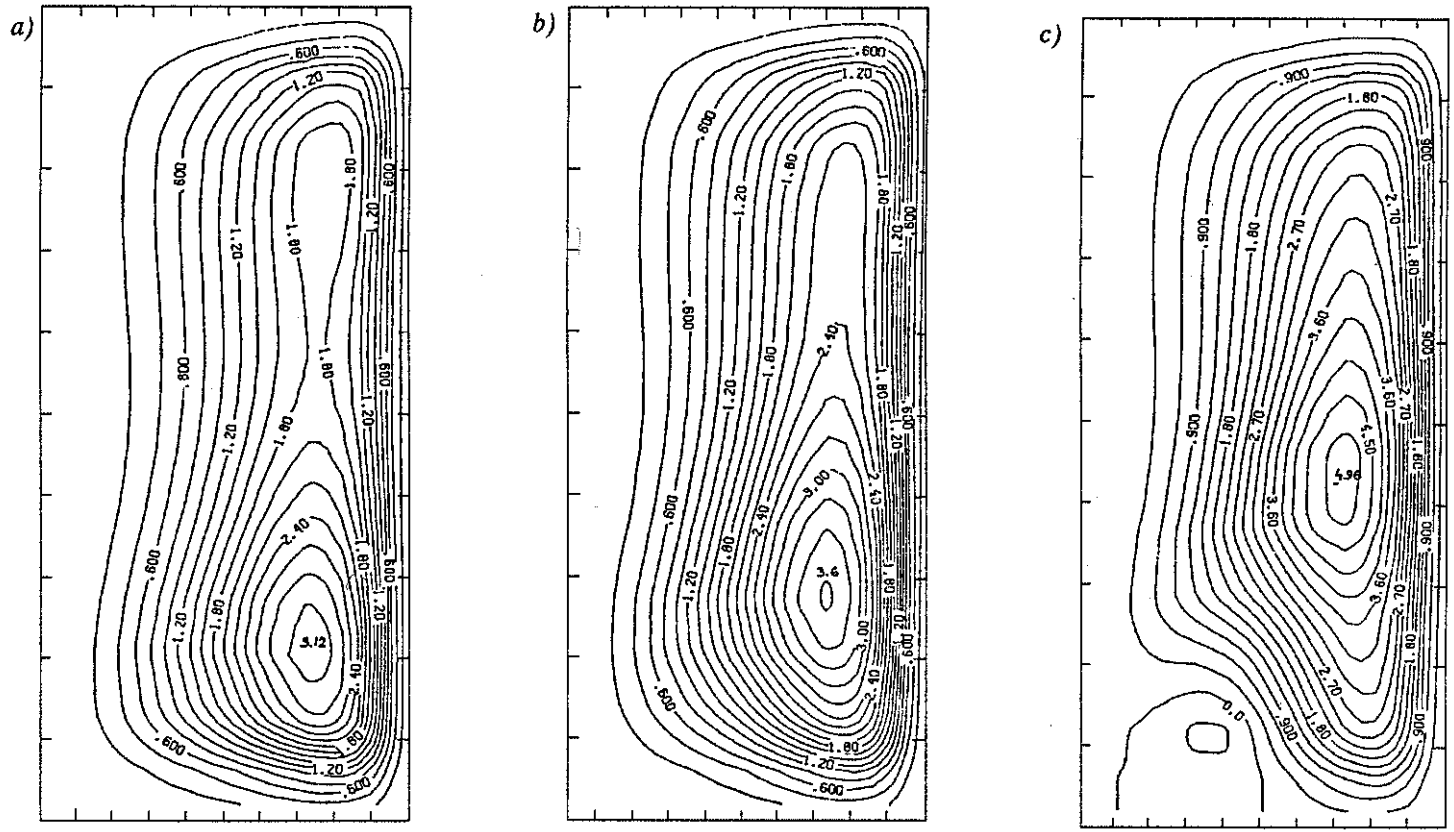

FIG. 3. Streamline patterns for different values of source power: a) 70 W, b) 60 W, c) 50 W. Mean pressure: $\overline{p} = 1$ ata. Cavity dimensions: Radius: $R_d = 1.8$ cm, height: $Z_d = 4.0$ cm. Source dimensions: Radius: $R_Q = 0.2$ cm, height: $Z_Q = 0.8$ cm.

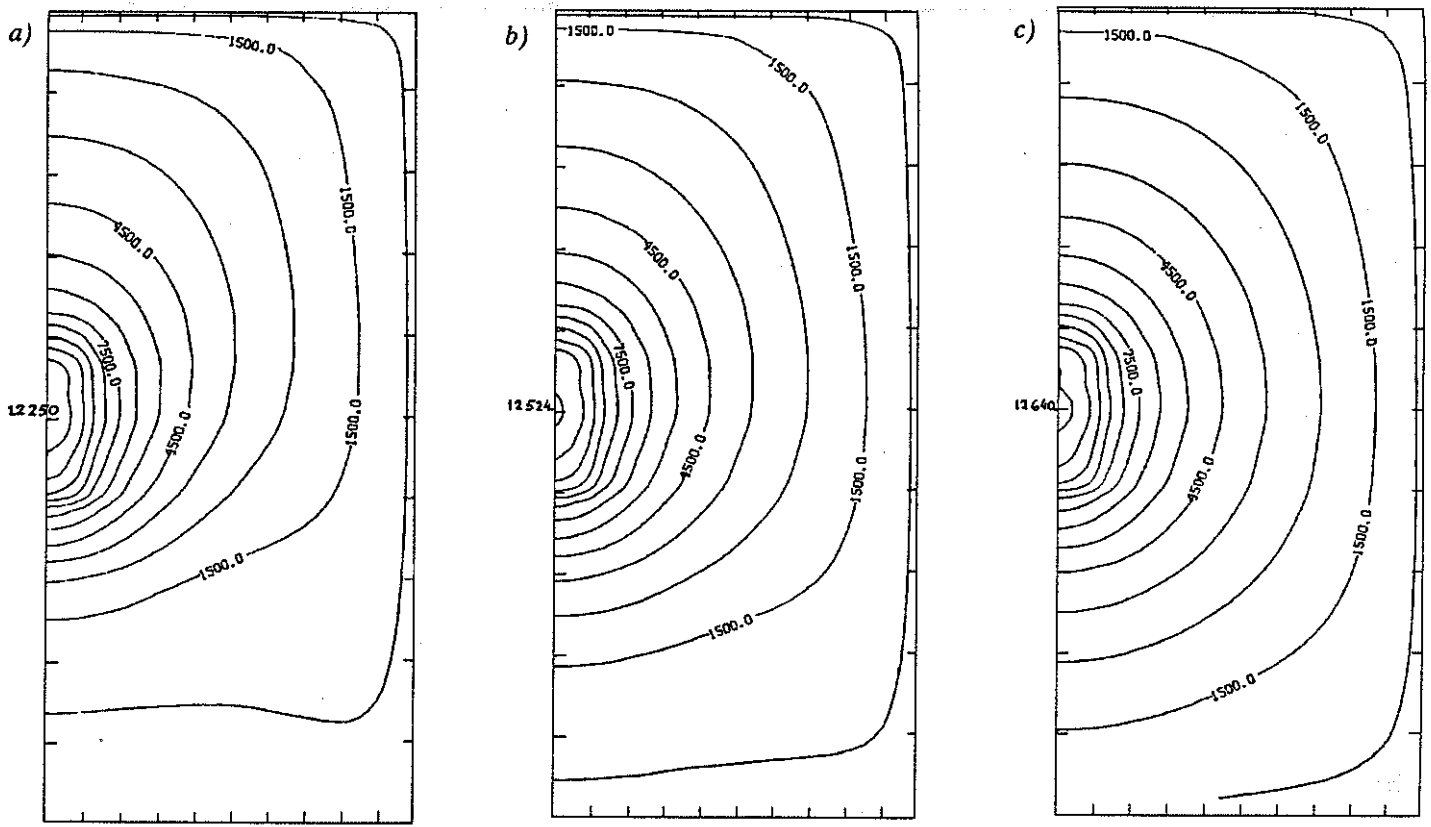

T_{max} = 12 250 K Re = 102
v_{max} = 45.5 cm/s Pe = 2.6

T_{max} = 12 524 K Re = 67
v_{max} = 32.7 cm/s Pe = 1.7

T_{max} = 12 640 K Re = 32
v_{max} = 21.0 cm/s Pe = 0.8

FIG. 4. Temperature contours for different values of mean pressure: a) 1 ata, b) 0.75 ata, c) 0.5 ata. Source power: $Q = 60$ W, Cavity dimensions: Radius: $R_d = 1.8$ cm, height: $Z_d = 4.0$ cm. Source dimensions: Radius: $R_Q = 0.2$ cm, height: $Z_Q = 0.8$ cm.

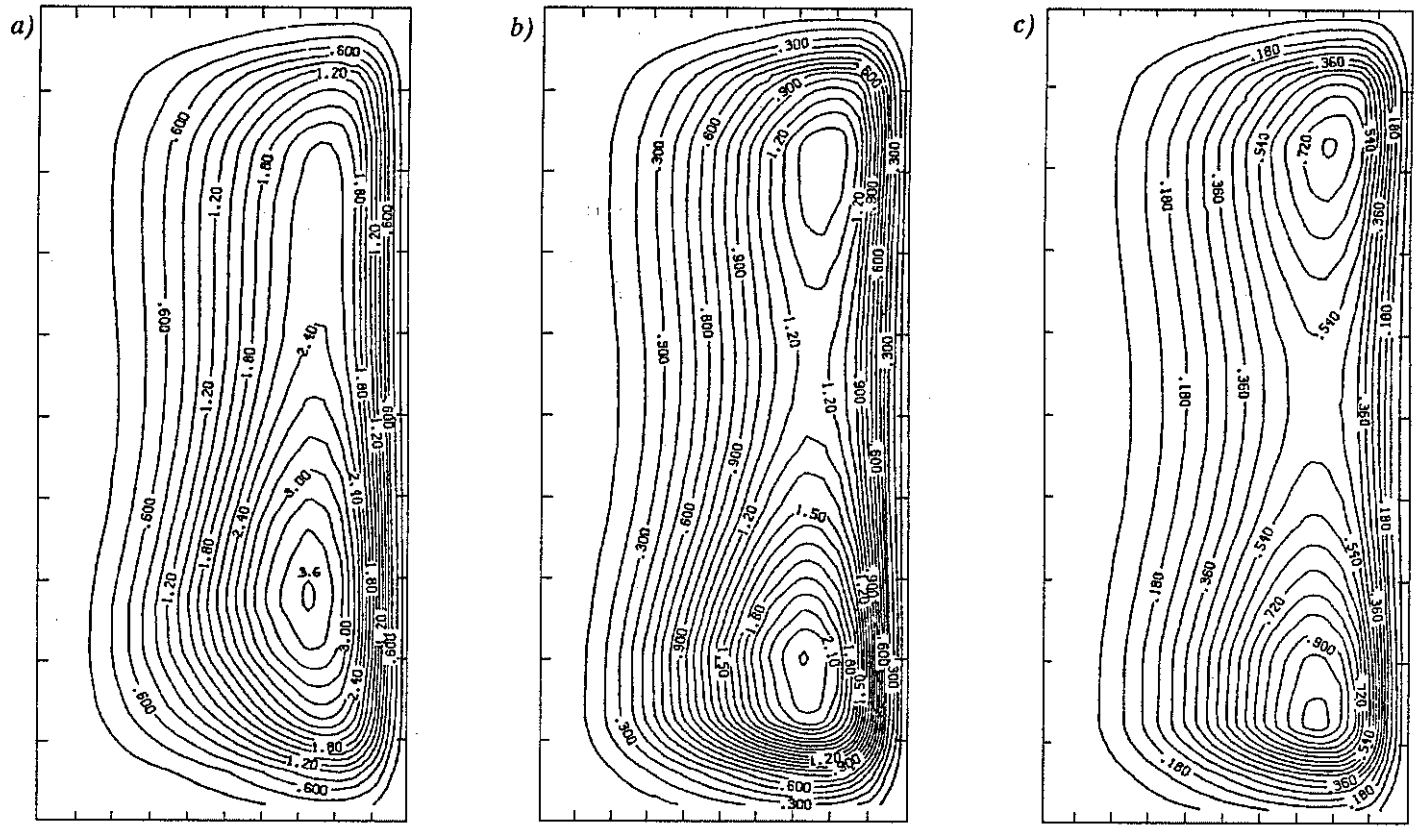

FIG. 5. Streamline patterns for different values of mean pressure: a) 1 ata, b) 0.75 ata, c) 0.5 ata. Source power: $Q = 60$ W. Cavity dimensions: Radius: $R_d = 1.8$ cm, height: $Z_d = 4.0$ cm. Source dimensions: Radius: $R_Q = 0.2$ cm, height: $Z_Q = 0.8$ cm.

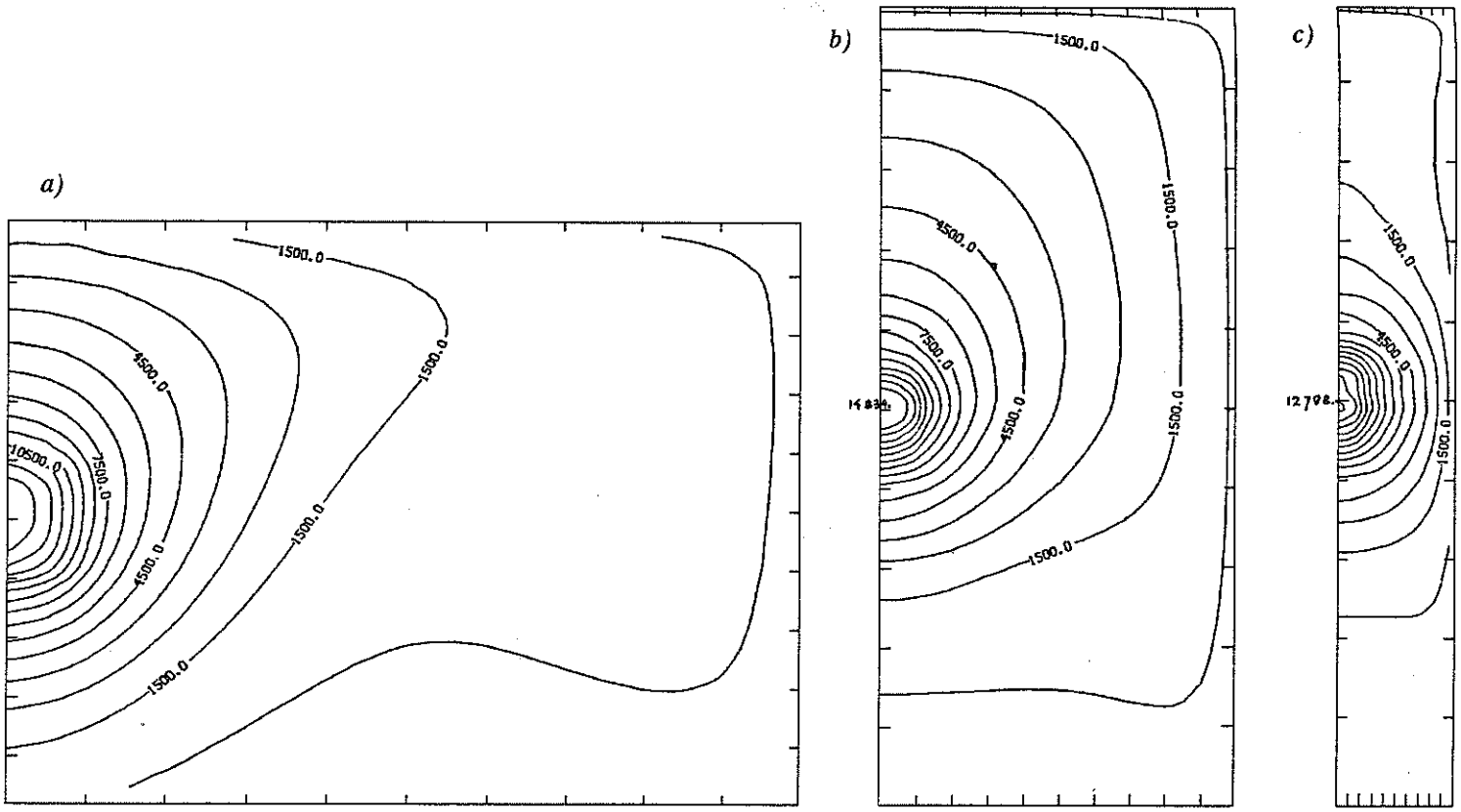

T_{max} = 14 469 K Re = 119
v_{max} = 67.6 cm/s Pe = 2.6

T_{max} = 14 834 K Re = 101
v_{max} = 49.7 cm/s Pe = 2.6

T_{max} = 12 788 K Re = 237
v_{max} = 31.9 cm/s Pe = 7.4

FIG. 6. Temperature contours for different values of aspect ratio: a) $a/3$, b) a, c) $3a$. Source power: 60 W. Mean pressure: $\overline{p} = 1$ ata. Cavity dimensions: a) $R_d = 2.7$ cm, $Z_d = 2.0$ cm; b) $R_d = 1.8$ cm, $Z_d = 4.0$ cm; c) $R_d = 0.9$ cm, $Z_d = 6.0$ cm. Source dimensions: Radius: $R_Q = 0.2$ cm, height: $Z_Q = 0.8$ cm.

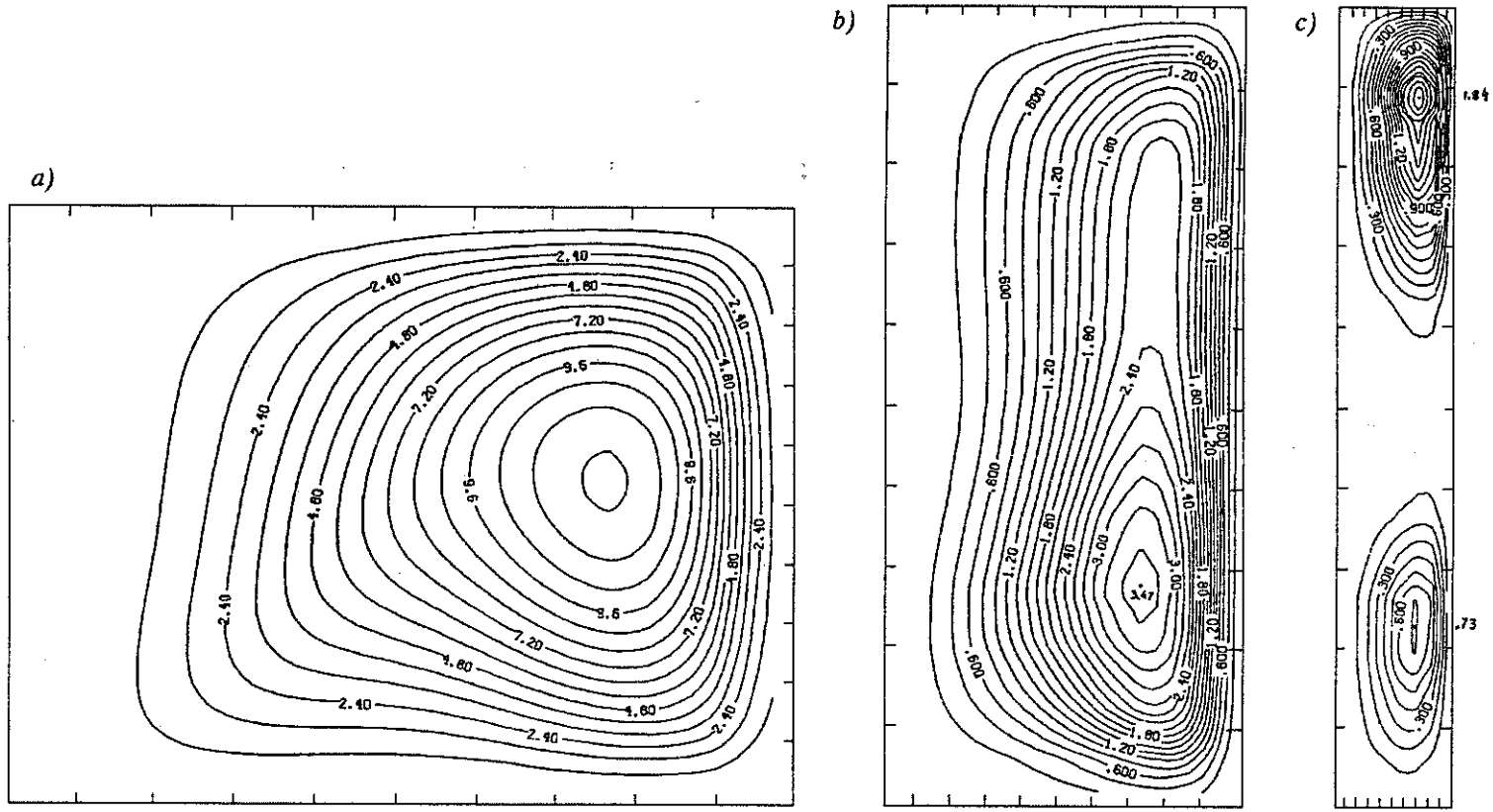

T_{max} = 14 469 K Re = 119
v_{max} = 67.6 cm/s Pe = 2.6

T_{max} = 14 834 K Re = 101
v_{max} = 49.7 cm/s Pe = 2.6

T_{max} = 12 788 K Re = 237
v_{max} = 31.9 cm/s Pe = 7.4

FIG. 7. Streamline patterns for different values of aspect ratio: a) $a/3$, b) a, c) $3a$. Source power: 60 W. Mean pressure: $\overline{p} = 1$ ata. Cavity dimensions: a) $R_d = 2.7$ cm, $Z_d = 2.0$ cm; b) $R_d = 1.8$ cm, $Z_d = 4.0$ cm; c) $R_d = 0.9$ cm, $Z_d = 6.0$ cm. Source dimensions: Radius: $R_Q = 0.2$ cm, height: $Z_Q = 0.8$ cm.

The third comparison involves cavities of different aspect ratios. The shallow cavity (case a, aspect ratio: $a/3$) is of 2 cm height and 5.4 cm in diameter. The dimensions of the standard cavity (case b, aspect ratio: a) were given earlier in this section. The tall cavity (case c, aspect ratio: 3a) is 6 cm high and its diameter is 1.8 cm. The source heat-rate (60 W), the source dimensions (height = 0.4 cm, diameter = 0.4 cm), and the mean value of pressure (1 ata) are the same for the three cases. Temperature contours are shown in Fig. 6. Streamlines patterns (cf. Fig. 7) for the shallow and the standard cavity are topologically similar. In case c there is a characteristic split of the main vortex observed in many tall cavities with differentially heated vertical walls.

5. Conclusion

The numerical method presented in this paper was designed for a class of stationary convection flows that rarely become subject to theoretical and numerical analysis: incompressible but with a substantial variation of density. Allowing for high density gradients made the Boussinesq approximation inapplicable. The continuity and the momentum equations were therefore formulated in terms of primitive variables and pressure was eliminated as an active variable by applying the Stokes theorem to the momentum equation. In addition to eliminating pressure, the procedure – which involves taking a line integral of the momentum equation over a closed contour – provided some cancellation of terms representing the convective derivative in the momentum equation. This allowed for applying the numerical scheme designed for Navier–Stokes equations to problems with a cell Reynolds number higher than two, without using upwind differencing for the convective term. Among other attributes of the method, natural boundary conditions for main variables may be mentioned. Since primitive variables were used and, at the same time, pressure was eliminated, there was no need for setting boundary conditions for either vorticity or pressure. The continuity equation has been solved directly in each mesh.

Since the method was designed for a special class of problems, the range of its applicability is not easily extendable. To deal with compressible or three-dimensional flows, major modifications of the approach would be needed. In addition, line integration of the momentum equation over a contour resulted in a 12-point formula for velocity which is rather bulky as

compared to the standard 5-point formula. Still, for variable-density incompressible flows analyzed in two dimensions the method – based on a novel treatment of the momentum equation – may provide a convenient alternative to those methods accounting for variable density which were designed for compressible flows.

REFERENCES

1. W.ARTER, *Nonlinear Rayleigh-Bérnard convection with square planform*, J. Fluid Mech., **152**, 391–418, 1985.
2. A.BARANOWSKI, Z.MUCHA and Z.PERADZYŃSKI, *Experimental and theoretical study of the stability of continuous optical discharge in gases*, Adv. Mech., **1**, 125–147, 1978.
3. K.R.BLAKE, D.POULIKAKOS and A.BEJAN, *Natural convection near 4° C in a horizontal water layer heated from below*, Phys. Fluids, **27**, 2608–2616, 1984.
4. F.H.BUSSE and H.FRICK, *Square-pattern convection in fluids with strongly temperature-dependent viscosity*, J. Fluid Mech., **150**, 451–465, 1985.
5. R.COURANT, E.ISAACSON and M.REES, *On the solution of nonlinear hyperbolic differential equations by finite differences*, Comm. Pure Appl. Math., **5**, 243–255, 1952.
6. J.FROMM, *The time-dependent flow of an incompressible viscous fluid*, Methods Computat. Phys., **3**, 345–382, 1964.
7. N.A.GENERALOV, V.P.ZIMAKOV, G.I.KOZLOV, V.A.MASYUKOV and YU.P.RAIZER, *Experimental investigation of continous optical discharge*, Soviet Physics JETP, **34**, 763–769, 1972 [Originally published in Russian: Zh. Eksp. Teor. Fiz., **61**, 1434–1446, 1971].
8. B.GILLY, B.ROUX and P.BONTOUX, *Influence of thermal wall conditions on the natural convection in heated cavities*, [in:] R.W.LEWIS, K.MORGAN and B.A.SCHREFLER [Eds.], Numerical Methods in Heat Transfer, vol. 2, pp. 205–225, Wiley, New York 1983.
9. E.H.HIRSCHEL and A.GROH, *Wall-compatibility condition for the solution of the Navier-Stokes equations*, J. Computat. Phys., **53**, 346–350, 1984.
10. H.INABA and T.FUKUDA, *Natural convection in an inclined square cavity in regions of density inversion of water*, J. Fluid Mech., **142**, 363–381, 1984.
11. M.V.KARVE and Y.YALURIA, *Numerical simulation of the conjugate heat transfer process from a heated moving surface*, [in:] G.YAGAWA and S.N.ATLURI [Eds], Computational Mechanics'86, vol. 2, pp. VIII.19–24. Springer-Verlag, Tokyo-Berlin-Heidelberg-New York 1986.
12. S.KIMURA and A.BEJAN, *Natural convection in a differentially heated corner region*, Phys. Fluids, **28**, 2980–2989, 1985.

13. R.W.KNIGHT and M.E.PALMER III, *Simulation of free convection in multiple layers in an enclosure by finite differences*, [in:] M.S.SHIH [Ed.], Numerical Properties and Methodologies in Heat Transfer, pp. 305–319, Hemisphere, Washington, D.C., 1983.

14. G.I.KOZLOV, V.A.KUZNETSOV and V.A.MASYUKOV, *Radiative losses by argon plasma and the emissive model of a continuous optical discharge*, Soviet Physics JETP, **39**, 463–468, 1974 [Originally published in Russian: Zh. Eksp. Teor. Fiz. **66**, 954–964, 1974].

15. Y.LEE and S.KORPELA, *Multicellular natural convection in a vertical slot*, J. Fluid Mech., **126**, 91–121, 1983.

16. G.D.MALLINSON, A.D.GRAHAM and G.DE VAHL DAVIS, *Three-dimensional flow in a closed thermosyphon*, J. Fluid Mech., **109**, 259–275, 1981.

17. C.D.MOODY, *Maintenance of a gas breakdown in argon using* $10.6-\mu$ *cw radiation*, J. Appl. Phys., **46**, 2475–2482, 1975.

18. Z.MUCHA, Z.PERADZYŃSKI and A.BARANOWSKI, *Instability of continuous optical discharge*, Bull. Acad. Pol. Sci., **25**, 361–367, 1977.

19. P.J.O'ROURKE and F.V.BRACCO, *Two scaling transformations for the numerical computation of multidimensional unsteady laminar flames*, J. Computat. Phys., **33**, 185–203, 1979.

20. S.V.PATANKAR, *Numerical Heat Transfer and Fluid Flow*, Hemisphere, Washington and McGraw-Hill, New York-London 1980.

21. T.N.PHILIPS, *Natural convection in an enclosed cavity*, J. Computat. Phys., **54**, 365–381, 1984.

22. P.LE QUERE and A.T.DE ROQUEFORT, *Computation of natural convection in two-dimensional cavities with Chebyshev polynomials*, J. Computat. Phys., **57**, 210–228, 1985.

23. C.QUON, *Effects of grid distribution on the computation of high Rayleigh number convection in a differentially heated cavity*, [in:] T.M.SHIH [Ed], Numerical Properties and Methodologies in Heat Transfer, pp. 261–281, Hemisphere, Washington, D.C. 1983.

24. A.RAMARAJU, A.G.MARATHE and S.K.BISWAS, *Time accurate temperature history due to moving source of heat*, [in:] G.YAGAWA and S.N.ATLURI [Eds.], Computational Mechanics'86, vol. 2, pp. VIII. 45–50, Springer-Verlag, Tokyo-Berlin-Heidelberg-New York, 1986.

25. J.D.RAMSHAW, P.J.O'ROURKE and L.R.STEIN, *Pressure gradient scaling method for fluid flow with nearly uniform pressure*, J. Computat. Phys., **58**, 361–376, 1985.

26. P.J.ROACHE, *Computational Fluid Dynamics* (First edition, 1972), Hermosa, Albuquerque, N.M. 1976.

27. P.J.ROACHE, *The LAD, NOS and Split NOS methods for the steady-state Navier-Stokes equations*, Computers and Fluids, **3**, 179–195, 1978.

28. M.N.ROPPO, S.H.DAVIS and S.ROSENBLAT, *Bénard convection with time-periodic heating*, Phys. Fluids, **27**, 796–803, 1984.

29. S.G.RUBIN, *Incompressible Navier-Stokes and parabolized Navier-Stokes formulations and computational techniques*, [in:] W.G.HABASHI [Ed.], Computational Methods in Viscous Fluids (vol. 3 of Recent Advances in Numerical Methods), pp. 55–99, Pineridge Press, Swansea 1984.

30. J.SŁOMCZYŃSKA and Z.PERADZYŃSKI, *Finite-difference scheme for stationary Navier-Stokes equations with variable coefficients*, [in:] R.L.STERNBERG, A.J.KALINOWSKI and J.S.PAPADAKIS [Eds.], Nonlinear Partial Differential Equations in Engineering and Applied Science, pp. 343–376, M.Deker, New York 1980.

31. J.SŁOMCZYŃSKA, *A finite-difference method for a problem of stationary free convection caused by a strong heat source*, [in:] G.YAGAWA and S.N.ATLURI [Eds.], Computational Mechanics'86, vol. 2, pp. VIII.183–188, Springer-Verlag, Tokyo-Berlin-Heidelberg-New York 1986.

32. K.C.STENGEL, D.S.OLIVER and J.R.BOOKER, *Onset of convection in a variable-viscosity fluid*, J. Fluid Mech., **120**, 411–431, 1982.

33. I.C.WALTON, *The effect of shear flow on convection in a layer heated non-uniformly from below*, J. Fluid Mech., **154**, 303–319, 1985.

POLISH ACADEMY OF SCIENCES
INSTITUTE OF FUNDAMENTAL TECHNOLOGICAL RESEARCH.

Received March 16, 1993.